The Journal of Experimental Biology 207, 2157-2172
Published by The Company of Biologists 2004
doi:10.1242/jeb.00989

Structural colouration of mammalian skin: convergent evolution of coherently scattering dermal collagen arrays

Richard O. Prum[1,*] and Rodolfo H. Torres[2]

[1]*Department of Ecology and Evolutionary Biology, and Peabody Museum of Natural History, Yale University, PO Box 208105, New Haven, CT 06520, USA* and [2]*Department of Mathematics, University of Kansas, Lawrence, KS 66045, USA*

*Author for correspondence (e-mail: richard.prum@yale.edu)

Accepted 15 March 2004

Summary

For more than a century, the blue structural colours of mammalian skin have been hypothesized to be produced by incoherent, Rayleigh or Tyndall scattering. We investigated the colour, anatomy, nanostructure and biophysics of structurally coloured skin from two species of primates – mandrill (*Mandrillus sphinx*) and vervet monkey (*Cercopithecus aethiops*) – and two species of marsupials – mouse opossum (*Marmosa mexicana*) and wooly opossum (*Caluromys derbianus*). We used two-dimensional (2-D) Fourier analysis of transmission electron micrographs (TEMs) of the collagen arrays in the primate tissues to test whether these structural colours are produced by incoherent or coherent scattering (i.e. constructive interference). The structural colours in *Mandrillus* rump and facial skin and *Cercopithecus* scrotum are produced by coherent scattering by quasi-ordered arrays of parallel dermal collagen fibres. The 2-D Fourier power spectra of the collagen arrays from *Mandrillus* and *Cercopithecus* reveal ring-shaped distributions of Fourier power at intermediate spatial frequencies, demonstrating a substantial nanostructure of the appropriate spatial frequency to produce the observed blue hues by coherent scattering alone. The Fourier power spectra and the observed reflectance spectra falsify assumptions and predictions of the incoherent, Rayleigh scattering hypothesis. Samples of blue *Marmosa* and *Caluromys* scrotum conform generally to the anatomy seen in *Mandrillus* and *Cercopithecus* but were not sufficiently well preserved to conduct numerical analyses. Colour-producing collagen arrays in mammals have evolved multiple times independently within the two clades of mammals known to have trichromatic colour vision. Mammalian colour-producing collagen arrays are anatomically and mechanistically identical to structures that have evolved convergently in the dermis of many lineages of birds, the tapetum of some mammals and the cornea of some fishes. These collagen arrays constitute quasi-ordered 2-D photonic crystals.

Key words: structural colour, mammal, blue, skin, collagen, coherent scattering, Rayleigh scattering, Tyndall scattering, 2-D photonic crystal.

Introduction

The colours of organisms are produced by molecular pigments or by the physical interactions of light waves with biological nanostructures. Structural colours, produced by the latter mechanism, are an important component of the phenotype of many animals (Fox, 1976; Herring, 1994; Parker, 1999) and even some plants (Lee, 1997).

The physical mechanisms of structural colour production are often described as being diverse (Fox, 1976; Nassau, 1983; Parker, 1999; Srinivasarao, 1999). However, most mechanisms of structural colour production can be well understood as consequences of light scattering at the interfaces of materials that differ in refractive index (for an exception in insect cuticle, see Neville and Caveney, 1969). Light-scattering mechanisms can be classified as either incoherent or coherent (Bohren and Huffman, 1983). Incoherent scattering is the differential scattering of light wavelengths by individual scatterers and is determined by the size, shape and refractive index without regard to the phase relationships among multiple waves scattered by different objects (Bohren and Huffman, 1983). By contrast, coherent scattering is differential scattering of light wavelengths from multiple objects and is determined by the phases of the scattered light waves (Prum and Torres, 2003a,b).

Rayleigh scattering (also known as Tyndall scattering; see Young, 1982) is an incoherent scattering mechanism that predicts the production of short-wavelength hues – blue, violet, and ultraviolet – by diffuse, cloudy media or colloids. Coherent scattering can produce biological colours with a wide variety of different structures including thin films, crystal-like arrays and diffraction gratings. Unlike incoherent Rayleigh scattering, coherent scattering often produces the phenomenon of

iridescence – change in hue with angle of observation or illumination – because changes in angle of observation and illumination may affect the phase relationships among the scattered waves that determine the hue (Prum and Torres, 2003a,b). Consequently, since Mason (1923), iridescence has often been inaccurately synonymized with coherent scattering, and all noniridescent blue structural colours have been erroneously ascribed to incoherent Rayleigh or Tyndall scattering (Fox, 1976; Nassau, 1983; Lee, 1991, 1997; Herring, 1994).

Although it is correct that iridescent biological structural colours are produced exclusively by coherent scattering, we have demonstrated that a previously unappreciated class of nanostructural organization – quasi-ordered arrays – can produce noniridescent biological structural colours by coherent scattering alone (Prum et al., 1998, 1999a,b, 2003; Prum and Torres, 2003a,b). Quasi-ordered arrays have the unimodal distributions of scatterer size and spacing that can produce coherent scattering but that lack the laminar or crystal-like spatial organization at larger spatial scales that produces iridescence. We have identified coherently scattering quasi-ordered arrays in the spongy medullary keratin of structurally coloured feather barbs (Prum et al., 1998, 1999b, 2003) and the dermal collagen arrays (Prum et al., 1999a; Prum and Torres, 2003a) of various avian clades.

In order to analyze colour production by quasi-ordered tissues and the evolution of colour-producing arrays among the quasi-ordered, crystal-like and laminar organizations, we have developed a tool that uses the two-dimensional (2-D) Fourier transform of transmission electron micrographs of the colour-producing biological structures to characterize the periodicity of spatial variation in refractive index in these materials (Prum et al., 1998, 1999a,b; Prum and Torres, 2003a,b). The Fourier methods can test the fundamental incoherent scattering assumption of scatterer spatial independence and predict the reflectance spectrum produced by coherent light scattering from these arrays.

Recently, new photonic methods have begun to be applied to the study of biological structural colour production (Parker et al., 2001; Li et al., 2003; Sundar et al., 2003; Vukusic, 2003; Vukusic and Sambles, 2003). We conclude with a discussion of colour-producing collagen arrays as two-dimensional photonic crystals and a comparison between photonic methods and the Fourier method applied here.

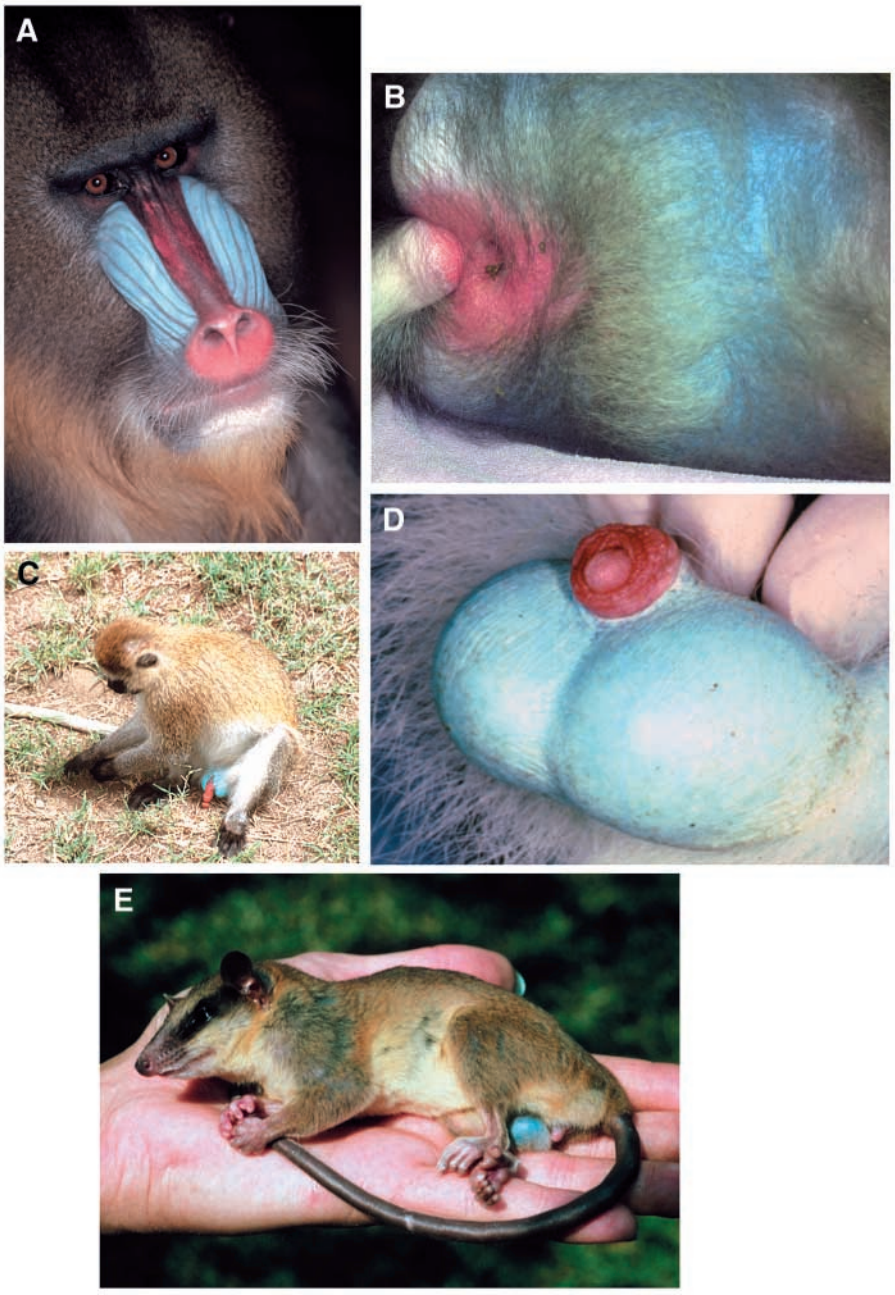

Fig. 1. Structurally coloured skin of mammals examined. (A) Male mandrill (*Mandrillus sphinx*) blue facial skin (reproduced with permission from Corbis Photo). (B) Male mandrill blue rump skin (reproduced with permission from Jay Peterson). (C) Male vervet monkey (*Cercopithecus aethiops pygerythrus*) with vividly blue scrotum (reproduced with permission from Roland Kays). (D) Close-up of the blue scrotum of a vervet monkey (*C. a. pygerythrus*; reproduced with permission from Dr Kenneth Soike). (E) Male mouse opossum (*Marmosa robinsoni*) with blue scrotum (reproduced with permission from Louise Emmons). Photo depicts a species that is closely related to the species examined (*M. mexicana*).

Table 1. *Measurements and predictions from the primate specimens analyzed*

Sample	Observed colour	Peak reflectance (nm)	Peak spatial frequency (nm^{-1})	Modal interfibre distance (nm)	Peak predicted reflectance (nm)	Prediction error (nm)	Sample size
Mandrillus sphinx							
Male face (A24)	Light blue	467	0.00646	154	430	37	14
Male face (A23)	Light blue	458	0.00547	182	490	32	20
Male rump (A25)	Dark blue	378	0.00666	150	410	32	39
Male rump (A22)	Dark blue	387	0.00726	138	390	3	29
Female face (A20)	Light blue	490	0.00686	146	460	30	30
Female face (A21)	Light blue	491	0.00786	127	360	131	19
Cercopithecus aethiops sabaeus							
Scrotum (A09)	Pearly blue	506	0.00428	233	760	260	6
Cercopithecus aethiops pygerythrus							
Scrotum (A13)	Vivid blue	~475*	0.00587	170	400	~75	7

*Reflectance data for *Cercopithecus aethiops pygerythrus* from Findlay (1970).

Structural colour production in mammals

In contrast with invertebrates and other vertebrate classes, integumentary structural colouration is rare in mammals (Fox, 1976). In all, violet, blue or green skin is known from only a few genera in the orders of marsupials and primates (Fig. 1). For over 100 years, with rare exception, the structural colours in the skin of mammals have been attributed to Rayleigh or Tyndall scattering (Camichel and Mandoul, 1901; Hill, 1970; Fox, 1976; Price et al., 1976; Nassau, 1983; Rees and Flanagan, 1999; Reisfeld, 2000). Findlay (1970) criticized the Tyndall scattering hypothesis but proposed a vague and physically inexplicit alternative. Oettlé (1958), however, hypothesized explicitly that the vivid blue colour of the scrotum of the vervet monkey (*Cercopithecus aethiops*) is produced by coherent scattering (i.e. constructive interference) by dermal collagen. Using a series of elegant light microscope observations, Oettlé documented that expanding the blue scrotum tissue with formic acid and heat resulted in a shift in the colour to longer, reddish wavelengths. Oettlé's observation provided strong evidence for coherent scattering, but his ground-breaking paper has not been broadly cited.

To our knowledge, Price et al. (1976) is the only previous publication to use transmission electron microscopy (TEM) to examine structurally coloured mammal skin. However, Price et al. (1976) focused on the distribution of melanin in the skin and did not examine the nanostructure of the dermal collagen. They concluded that the blue hue of the scrotum of *C. aethiops* was produced by Tyndall scattering above a layer of melanocytes (Price et al., 1976).

We used fibre-optic spectrophotometry, light microscope histology, transmission electron microscopy (TEM) and 2-D Fourier analysis of TEM images to investigate structurally coloured skin from four species of mammals: the mandrill, *Mandrillus sphinx*, and the vervet monkey, *C. aethiops* (Cercopithecidae; Primates); and the mouse opossum, *Marmosa mexicana*, and the wooly opossum, *Caluromys derbianus* (Didelphidae; Marsupialia). We found that structural colours of mammal skin are produced by coherent scattering from quasi-ordered arrays of dermal collagen fibres. These arrays are exactly convergent with colour-producing collagen that has evolved numerous independent times in the skin of birds (Prum and Torres, 2003a), in the tapetum fibrosum of the sheep eye (Bellairs et al., 1975) and in the iridescent corneal stroma of certain fishes (Lythgoe, 1974).

Materials and methods

We examined 3 mm-diameter biopsies of structurally coloured light blue facial and dark blue rump skin of two adult male and two adult female mandrill, *Mandrillus sphinx* L. (Fig. 2; Table 1), courtesy of the Brookfield Zoo, Chicago, IL, USA. We also examined two specimens of the scrotum skin from male vervet monkey, *Cercopithecus aethiops* L. (Fig. 2; Table 1), from the Tulane Primate Research Center, Covington, LA, USA. The first specimen was from an individual with a bright blue scrotum of East African origin (*C. a. pygerythrus*; Fig. 1), and the second specimen was from an individual with a light, pearly blue scrotum from a feral Caribbean population of West African origin (*C. a. sabaeus*). We also examined single blue scrotum specimens of the mouse opossum (*Marmosa mexicana* Merrian) and wooly opossum (*Caluromys derbianus* Waterhouse) from Costa Rica, courtesy of Robert M. Timm.

Specimens of *Mandrillus* and the pearly blue specimen of *Cercopithecus* were fixed in 2.5% glutaraldehyde or in Karnovsky's fixative (2.5% glutaraldehyde, 2.5% paraformaldehyde) for 12 h and then stored in cacodylate buffer. The first specimen of vividly blue scrotum from *C. a. pygerythrus* was frozen for several months before fixation in 2.5% glutaraldehyde. The *Marmosa* specimens were fixed and stored in 10% formalin, and the *Caluromys* specimen was fixed originally in 70% ethanol. The marsupial specimens were fixed

again in Karnovsky's fixative for 2 h at 4°C before microscopy but were not sufficiently well preserved for numerical analysis of collagen nanostructure.

The reflectance spectra of all *Mandrillus* specimens and the pearly blue *Cercopithecus* specimen were measured using an Ocean Optics S2000 fibre optic diode array spectrometer with an Ocean Optics PX-2 pulsed xenon light source (Ocean Optics, Dunedin, FL, USA). This spectrometer produces 2048 reflectance data points between 160 nm and 865 nm (or 1520 data points between 300 nm and 800 nm) with an average error of 0.14 nm. Measurements were made with perpendicularly incident light from 6 mm away, producing an illuminated field of approximately 3 mm^2 with 100–500 ms summation time. A Spectralon diffuse reference standard from Ocean Optics was used as a white standard, and the ambient light of a darkened room was used as a dark reference. Percent reflectance was calculated in a standard fashion (Prum et al., 1999a). Reflectance spectra were recorded from the bluest available portion of each specimen. The vividly blue *C. a. pygerythrus* scrotum specimen was received before the reflectance spectrophotometry was available in our lab, and no measurements were made. However, reflectance spectra for this subspecies are reported by Findlay (1953, 1970) (see Table 1, Fig. 7H). The specimens of *Marmosa* and *Caluromys* did not preserve any visible or measurable colour and were not measured.

For light microscopy, samples of all species were embedded in paraffin, cut into 10 μm sections and stained with Masson's trichrome, which includes the collagen-specific stain fast-green. For TEM, skin samples were post-fixed in 2–4% osmium tetroxide for 1.5 h. They were then stained with 2% aqueous uranyl acetate for 1 h. Tissue pieces were then dehydrated through an ethanol series and embedded in Eponate 12. They were sectioned with a diamond knife to ~100 nm thick. Specimens were viewed with a JEOL EXII transmission electron microscope. TEM micrographs were taken with Polaroid negative film or were digitally captured using a Soft-Imaging Megaview II CCD camera (1024×1200 pixels). Numerical analyses were conducted directly on the digital images or on the photograph negatives after scanning at 300 dpi.

2-D Fourier analysis

Coherent scattering of visible wavelengths is a consequence of nanoscale spatial periodicity in refractive index of a tissue. Following a theory of corneal transparency by Benedek (1971), we have developed an application of the discrete Fourier 2-D transform to analyze the periodicity and optical properties of structural coloured tissue. Discrete Fourier analysis transforms a sample of data points into an equivalent sum of component sine waves of different frequencies and amplitudes (Briggs and Henson, 1995). The amplitudes of the Fourier component waves express the relative contribution of that frequency of variation to the periodicity of the original data. The variation in the squared amplitudes over all Fourier components is called the Fourier power spectrum. The relative values of the different Fourier components in the power spectrum express the comparative contribution of those spatial frequencies of variation to the original function. This application of Fourier analysis is derived independently from electromagnetic optical theory (Benedek, 1971) and is distinct from the traditional physical field of 'Fourier optics', although they both describe coherence among light waves.

The digital or digitized TEM images were analyzed using the matrix algebra program MATLAB (version 6.2; www.mathworks.com) on a Macintosh computer. The scale of each image (nm $pixel^{-1}$) was calculated from the number of pixels in the scale bar of the micrograph. The largest available square portion of each array was selected for analysis; for most images this area was 1024 $pixels^2$. The average refractive index of each tissue was estimated by generating a two-partition histogram of image darkness (i.e. the distribution of darker and lighter pixels). The frequency distribution of darker and lighter pixels was used to estimate the relative frequency of collagen and mucopolysaccharide in the image and to calculate a weighted average refractive index for the tissue. Previously, we have used estimates of the refractive indices of collagen and the mucopolysaccharide matrix between collagen fibres of 1.51 and 1.35, respectively (Prum et al., 1994, 1999a), taken from Maurice (1984). Recently, however, more refined methods have estimated the refractive indices of collagen as 1.42 and mucopolysaccharide as 1.35 (Leonard and Meek, 1997; Prum and Torres, 2003a).

The numerical computation of the Fourier transform was done with the well-established 2-D fast Fourier transform (FFT2) algorithm (Briggs and Henson, 1995). We calculated the 2-D Fourier power spectrum, or the distribution of the squares of the Fourier coefficients. The 2-D Fourier power spectrum resolves the spatial variation in refractive index in the tissue into its periodic components in any direction from a given point (Fig. 5). The 2-D Fourier power spectra are expressed in spatial frequency (nm^{-1}) by dividing the initial spatial frequency values by the length of the matrix (pixels in the matrix multiplied by nm $pixel^{-1}$). Each value in the 2-D power spectrum reports the magnitude of the periodicity in the original data of a specific spatial frequency in a given direction from all points in the original image. The spatial frequency and direction of any component in the power spectrum are given by the length and direction, respectively, of a vector from the origin to that point. The magnitude is depicted by the colour (from blue to red), but the units are dimensionless values related to the total darkness of the original digital images.

We calculated radial average power distributions from the power spectra using 100 spatial frequency bins, or annuli, between 0 and 0.02 nm^{-1} and normalized to % total Fourier power (Fig. 6). Composite radial average power distributions were calculated from a sample of power spectra from multiple TEM images to provide an indication of the predominant spatial frequency of variation in refractive index in the tissue over all directions (Table 1; Fig. 6).

We also produced predicted reflectance spectra based on the 2-D Fourier power spectra, image scales and average refractive indices (Fig. 7). First, a radial average of the power spectrum was calculated using concentric radial bins, or annuli,

corresponding to fifty 10 nm-wide wavelength intervals between 300 and 800 nm. The radial average power values were expressed in % visible Fourier power by normalizing the total power values across all potentially visible spatial frequencies (i.e. potentially scattering light between 300 and 800 nm) to 1. The inverse of the spatial frequency averages for each wavelength were then multiplied by twice the average refractive index of the medium and expressed in terms of wavelength (nm). A few images depict oblique, elliptical sections of the cylindrical collagen fibres, which will bias the predicted hue toward longer wavelengths. In these cases, the radial average was calculated from a single quadrant or from a custom radial section of the power spectrum that lacked the elliptical distortion. Composite predicted reflectance spectra for each tissue were produced by averaging the normalized predicted spectra from a sample of TEM images (Fig. 7). The result is a theoretical prediction of the relative magnitude of coherent light scattering by the tissue that is based entirely on the spatial variation in refractive index of the tissue (Fig. 7; Table 1).

Results

Anatomy

Light microscope histology of *Mandrillus*, *Cercopithecus* and *Caluromys* revealed that the epidermis is thin (30–75 μm) and unpigmented (Fig. 2). The colour-producing dermis consisted of a thick layer of collagen – 1500 μm (*Mandrillus* face) or 800 μm (*Mandrillus* rump, *Cercopithecus* scrotum, *Caluromys* scrotum) – that stains vividly blue with Masson's trichrome (Fig. 2). In the blue rump skin of *Mandrillus* and the blue scrotum of *Cercopithecus*, there was a dense layer of melanocytes ~800 μm below the epidermis (Fig. 2B,C), but melanocytes were absent from the blue *Mandrillus* facial skin and scarce in the *Caluromys* scrotum (Fig. 2A,D).

Colour and spectrophotometry

Reflectance spectra of the skin samples revealed bright blue colours with distinct peak hues (Fig. 3). The reflectance peaks varied from 378 to 385 nm for male *Mandrillus* rump skin, 458

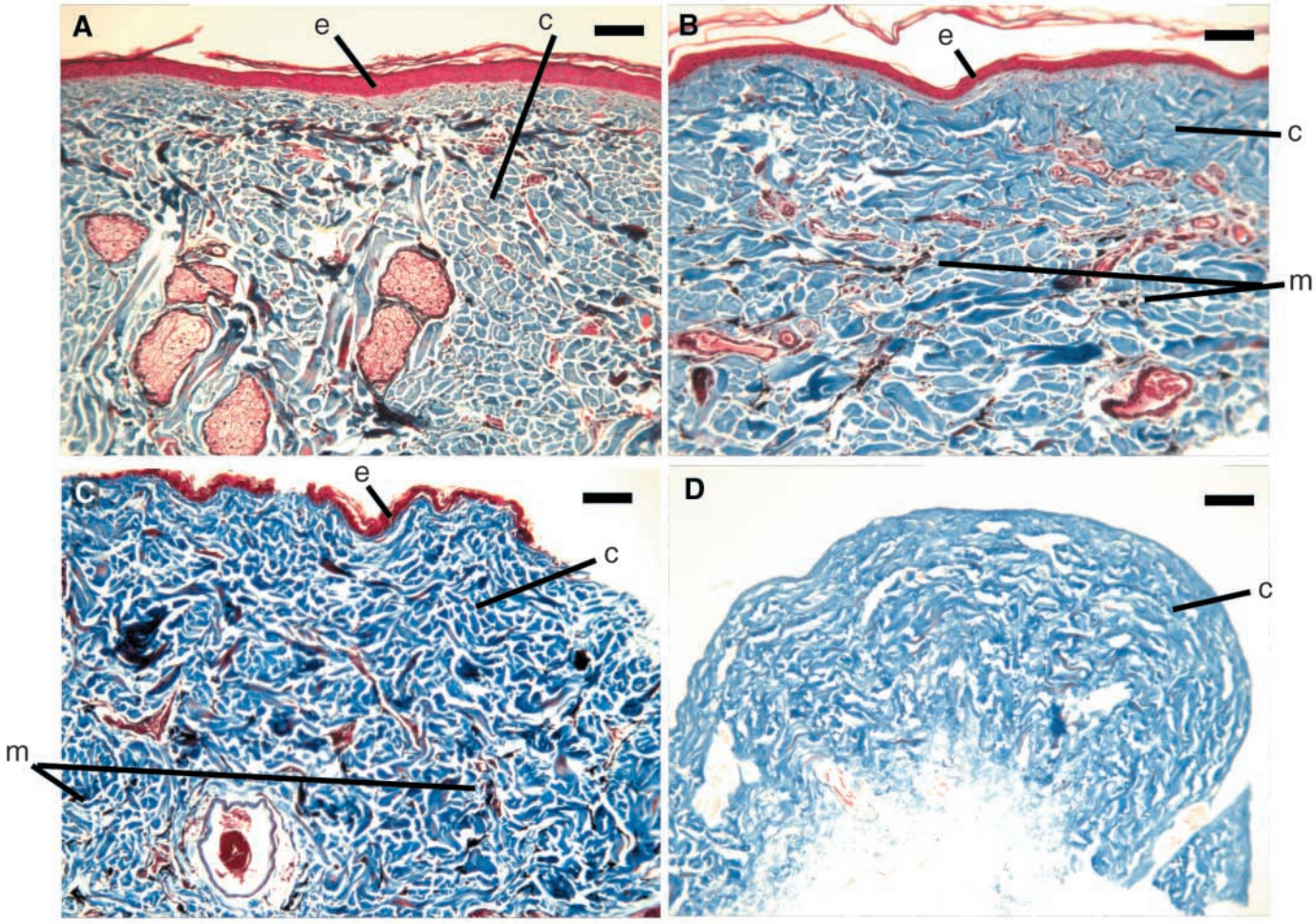

Fig. 2. Light micrographs of structurally coloured skin of (A) male mandrill (*Mandrillus sphinx*) facial skin; (B) male mandrill rump skin; (C) vervet monkey (*Cercopithecus aethiops*) scrotum and (D) wooly opossum (*Caluromys derbianus*) scrotum (epidermis detached and missing). All specimens were stained with Masson's trichrome, which stains collagen blue. All scale bars are 100 μm. Abbreviations: c, collagen; e, epidermis; m, melanin.

to 467 nm for male *Mandrillus* facial skin, 490 to 491 nm for female *Mandrillus* facial skin and 506 nm for the pearly blue *C. a. sabaeus* scrotum (Fig. 3). The reflectance spectrum of the vividly blue scrotum skin of *C. a. pygerythrus* was not measured here, but a scrotum reflectance spectrum from the same subspecies has been published by Findlay (1953, 1970) and shows a unimodal peak of 35% reflectance at approximately 475 nm (Fig. 7H). The scrotum skin of *Marmosa* and *Caluromys* were not sufficiently well fixed to preserve any measurable colour, but both species were medium blue at the time they were collected.

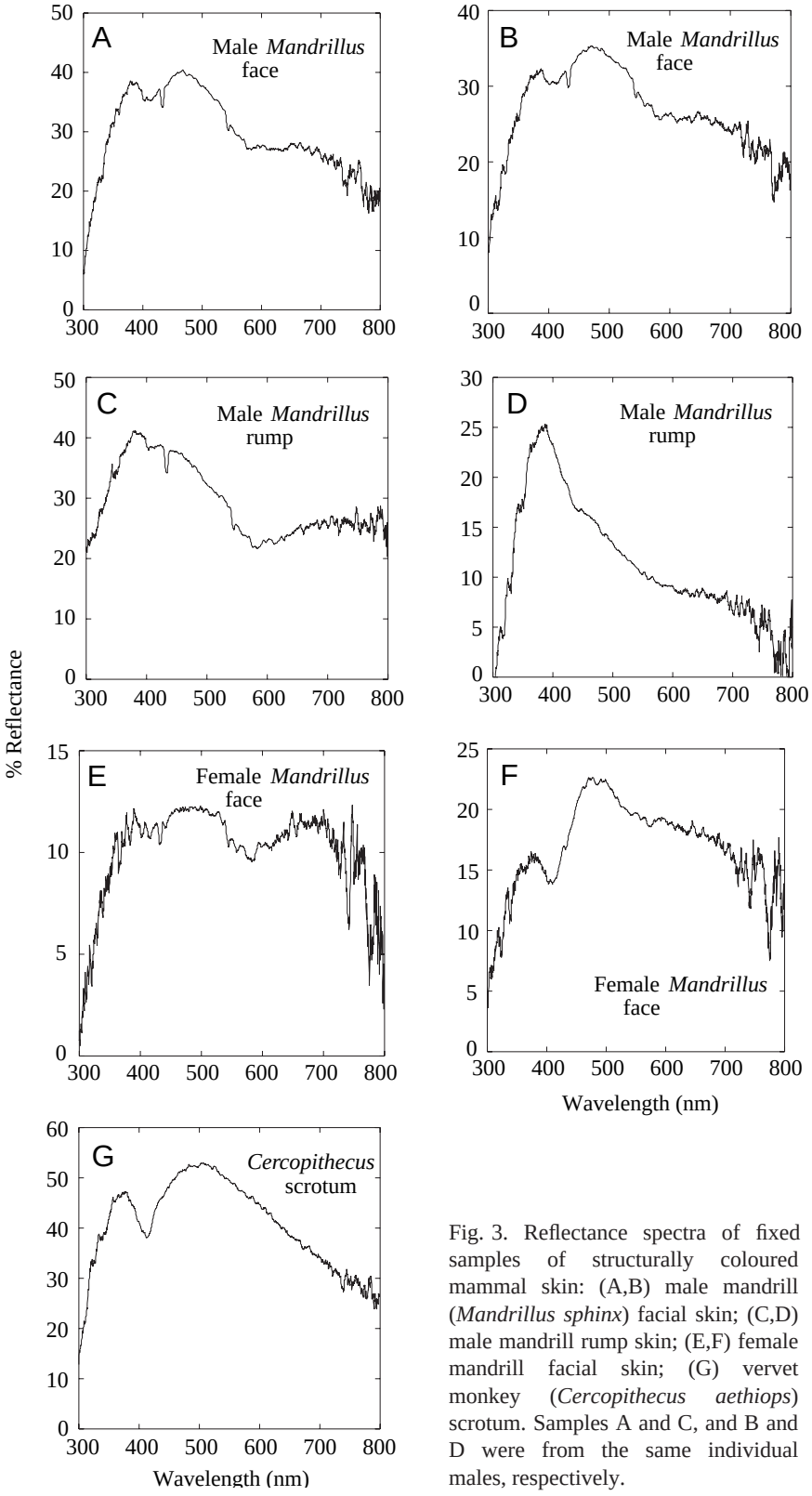

Fig. 3. Reflectance spectra of fixed samples of structurally coloured mammal skin: (A,B) male mandrill (*Mandrillus sphinx*) facial skin; (C,D) male mandrill rump skin; (E,F) female mandrill facial skin; (G) vervet monkey (*Cercopithecus aethiops*) scrotum. Samples A and C, and B and D were from the same individual males, respectively.

The blue colour of male *Mandrillus* facial skin was apparently more brilliant (40% peak reflectance) and saturated (purer in hue) than in female *Mandrillus* facial skin, which showed lower peak reflectance (12–22%) and substantial reflectance of longer wavelengths (i.e. less saturated in colour) (Fig. 3A,B,E,F).

Nanostructure

The colour-producing dermis of *Mandrillus*, *Cercopithecus*, *Marmosa* and *Caluromys* was composed of abundant parallel collagen fibres (Fig. 4). These collagen fibres form quasi-ordered arrays that are characterized by normal distribution of fibre diameters and nearest neighbour distances but that lack periodicity at larger spatial scales (Fig. 4). The *Caluromys* tissue examined was not sufficiently well fixed to preserve many of the details of collagen nanostructure.

Fourier analyses

The 2-D Fourier power spectra of TEMs of cross-sections of the colour-producing dermal collagen arrays from *Mandrillus* and *Cercopithecus* revealed ring-shaped distributions of high-power values at intermediate spatial frequencies (Fig. 5). These ring-shaped power distributions indicate that the collagen arrays are substantially nanostructured at intermediate spatial frequencies and are not randomly distributed in space as assumed by incoherent scattering models. The ring-shaped distributions of high Fourier power values also demonstrate that these collagen arrays are equivalently nanostructured in all directions perpendicular to the fibres, which constitutes the quasi-ordered type of organization that will produce a noniridescent structural colour by coherent scattering (Prum et al., 1998, 1999a,b; Prum and Torres, 2003a,b). Radial averages of the power spectra of the TEMs of *Mandrillus* and *Cercopithecus* indicate peak spatial

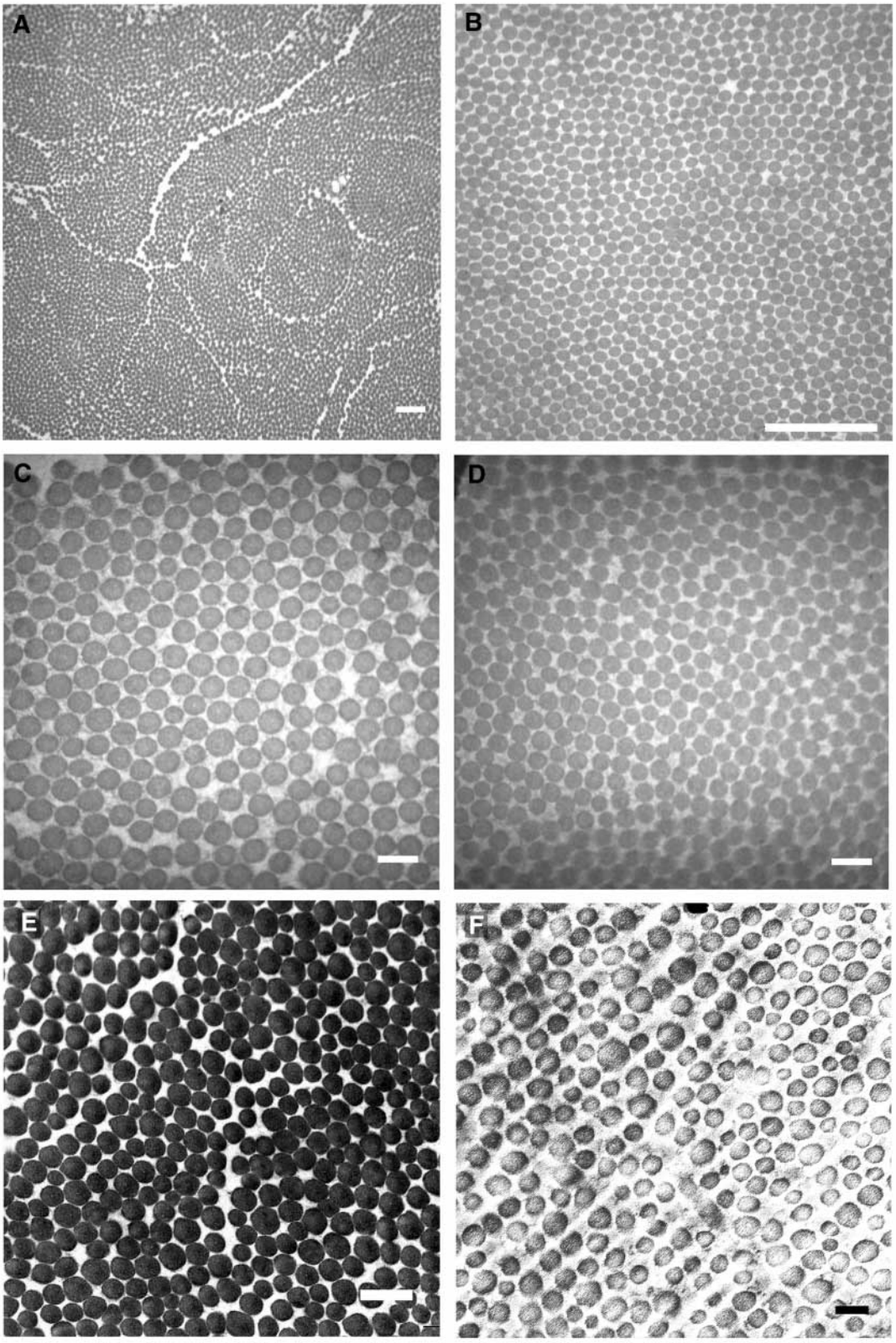

Fig. 4. Transmission electron micrographs of collagen arrays from structurally coloured mammal skin. (A) Female mandrill (*Mandrillus sphinx*) facial skin at 7500×. Scale bar, 500 nm. (B) Male mandrill rump skin at 25 000×. Scale bar, 1000 nm. (C) Male mandrill facial skin at 40 000×. Scale bar, 250 nm. (D) Male mandrill rump skin at 40 000×. Scale bar, 250 nm. (E) Vervet monkey (*Cercopithecus aethiops*) scrotum at 25 000×. Scale bar, 500 nm. (F) Mouse opossum (*Marmosa mexicana*) at 50 000×. Scale bar, 100 nm.

frequencies in refractive index variation that are appropriate for producing visible colours (Fig. 6; Table 1). These peak spatial frequencies correspond to modal distance between neighbouring collagen fibre centres of between 127 and 182 nm in *Mandrillus* and between 170 and 233 nm in *Cercopithecus* (Table 1).

The predicted reflectance spectra based on radial averages of the Fourier power spectra and the average refractive index

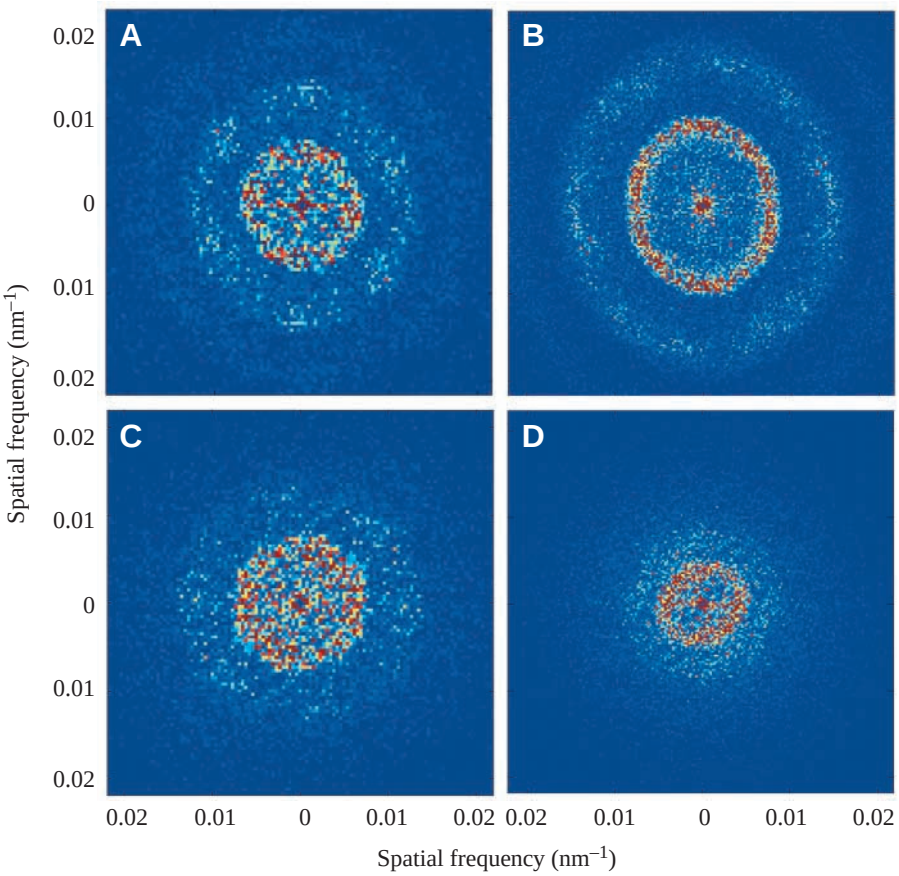

Fig. 5. Two-dimensional Fourier power spectra from transmission electron micrographs of colour-producing collagen arrays from: (A) male mandrill (*Mandrillus sphinx*) facial skin; (B) male mandrill rump skin; (C) female mandrill facial skin and (D) vervet monkey (*Cercopithecus aethiops*) scrotum. Colour scale (from blue to red) indicates the relative magnitude of the squared Fourier components, which are dimensionless quantities. Direction from the origin indicates the direction of the 2-D component waves in the image, and the distance from the origin indicates the spatial frequency (cycles nm^{-1}) of each Fourier component. The ring-shaped distribution of Fourier power demonstrates a predominant periodicity at intermediate spatial frequencies that is equivalent in all directions. The diameter of the ring is inversely proportional to the wavelength of the coherently scattered colour, so the power spectrum ring of the (A) light blue mandrill facial skin (Fig. 2A) has a smaller diameter than the (B) dark blue mandrill rump skin (Fig. 2C).

of these extracellular collagen arrays were closely congruent with the measured reflectance spectra for most samples of *Mandrillus* face and rump skin (Fig. 7; Table 1). For five of six *Mandrillus* samples, the error between the measured and the predicted peak reflectance varied between 3 and 37 nm, but one sample of female *Mandrillus* facial skin (A21) had a predicted peak reflectance of 360 nm, or 131 nm below the measured reflectance of 491 nm (Fig. 7F; Table 1). However, the predicted peak was quite close to the secondary peak of the reflectance spectrum of this specimen at 374 nm, within 14 nm (Fig. 7F).

We have not established the mechanism determining the secondary peak in some *Mandrillus* reflectance spectra. Each peak could be produced by a class of appropriately sized collagen arrays, and the relative size of the two peaks could be produced by the relative abundance of the two spatial classes. Thus, the male *Mandrillus* rump reflectance could be produced predominantly or exclusively by the smaller spatial class (Fig. 7D), and the male *Mandrillus* facial colour could be produced predominantly by the larger spatial class. Some samples of TEM images appear to have sampled only the smaller (Fig. 7D,F) or the larger (Fig. 7B) spatial class, giving rise to errors in predicting the shape of the reflectance spectra. Alternatively, the reduced reflectance at ~400 nm could be caused by absorption by an unknown material (Prum and Torres, 2003a).

In *Cercopithecus*, the vividly blue sample predicted a unimodal reflectance spectrum at 400 nm with a peak that was ~75 nm below a previously published reflectance spectrum of the scrotum of this subspecies of 475 nm (Fig. 7H; Table 1; Findlay, 1953, 1970). However, the reflectance spectrum predicted for the pearly blue *Cercopithecus* scrotum sample featured broad reflectance above 500 nm, which was not congruent with measured reflectance of this specimen (Fig. 7G). However, the 'pearly' quality of the colour of this specimen to the eye indicates that it may have had some longer wavelength yellowish reflections. In making the reflectance measurements, we focused on the most bluish areas, perhaps creating a bias in the colour measurements that was not sampled by the TEM observations.

Discussion

An investigation of the colour, anatomy and nanostructure of structurally coloured skin of mandrill (*Mandrillus sphinx*) and vervet monkey (*Cercopithecus aethiops*) documents that these colours are produced by coherent scattering from quasi-ordered arrays of dermal collagen fibres. The dermal collagen arrays of *Mandrillus* and *Cercopithecus* are nanostructured at the appropriate spatial scale to produce the observed hues by coherent scattering alone (i.e. constructive interference among light waves scattered by adjacent collagen fibres). The differences in hue between different areas of skin are apparently due to the size and spacing of dermal collagen fibres

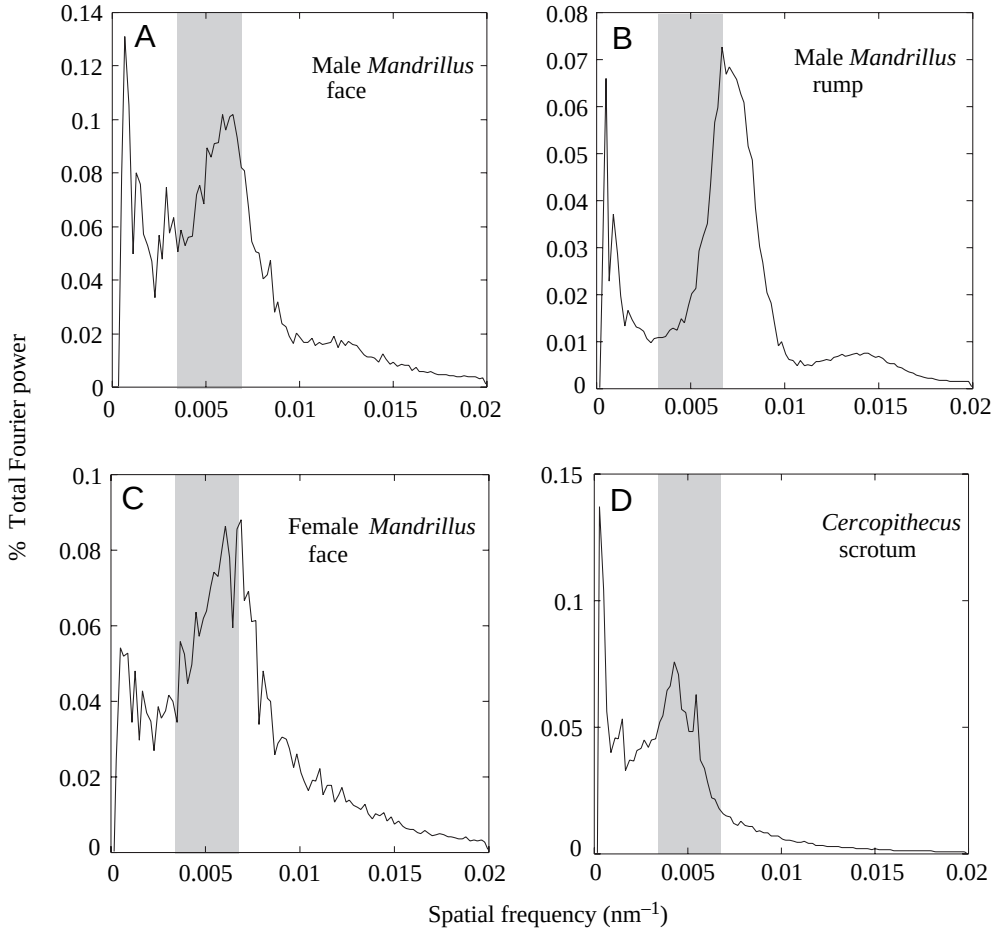

Fig. 6. Radial averages of power spectra from (A) male mandrill (*Mandrillus sphinx*) facial skin; (B) male mandrill rump skin; (C) female mandrill facial skin and (D) vervet monkey (*Cercopithecus aethiops*) scrotum. The shaded zone shows the range of spatial frequencies that are likely to produce mammal-visible coherent reflections, assuming a visible spectrum of 400–700 nm and an average refractive index in the dermis of 1.4. Peaks in the grey zone demonstrate that the predominant spatial periodicity of the collagen arrays is appropriate for the production of visible colours by coherent scattering. Sample sizes for each analysis are shown in Table 1.

(Prum et al., 1999a; Prum and Torres, 2003a,b). The ring-shaped Fourier power distributions demonstrate that this nanostructure is equivalent in all directions within the tissue perpendicular to the collagen fibres (Fig. 5), further explaining how these quasi-ordered arrays produce a non-iridescent colour by interference (Prum et al., 1998, 1999a,b; Prum and Torres, 2003a,b). The Fourier analyses of some samples were able to accurately predict the hue and shape of the specimen reflectance spectrum, but others were not as accurate (see Sources of error). However, the observed congruence is striking given that there are no reasons, other than nanostructuring for colour production, to expect these particular spatial frequencies to predominate within dermal collagen.

The Fourier analyses of blue *Mandrillus* and *Cercopithecus* skin also falsify the incoherent scattering hypotheses of colour production, including Rayleigh, Tyndall and Mie scattering. The spatial variation in refractive index in these arrays is not random over the spatial scale of visible light, as assumed by incoherent scattering models. Rather, the collagen arrays are highly nanostructured at precisely the spatial scale to create coherently scattered visible colours. Furthermore, the reflectance spectra of *Mandrillus* and *Cercopithecus* skin reveal peak hues in the visible or near-ultraviolet wavelengths and not the exponentially increasing reflectance into the ultraviolet that is predicted by the Rayleigh's inverse fourth power law (Bohren and Huffman, 1983).

Observations of the anatomy of the blue scrotum skin from *Marmosa mexicana* and *Caluromys derbianus* indicate that the same anatomy and physical mechanisms are responsible for structural colour production in these species, but the samples of these species were not sufficiently well preserved for quantitative analysis.

These analyses constitute the first demonstration of the physical mechanism of structural colour production in mammalian skin. For over 100 years, the structural colours of mammalian skin have been consistently attributed to incoherent, Rayleigh or Tyndall scattering (Camichel and Mandoul, 1901; Hill, 1970; Fox, 1976; Price et al., 1976; Rees and Flanagan, 1999; Reisfeld, 2000). This hypothesis survived virtually unchallenged for a century in a nearly complete absence of data because of the erroneous notion that all noniridescent, blue structural colours were produced by Rayleigh or Tyndall scattering. Oettlé (1958) was alone in proposing that the blue colour of the scrotum of *C. aethiops* is produced by coherent scattering. Oettlé also correctly identified the dermal collagen as the source of the colour. However, Oettlé (1958) did not test his hypothesis with any electron microscopic observations of the nanostructure of the tissue and published his observations in an obscure medical

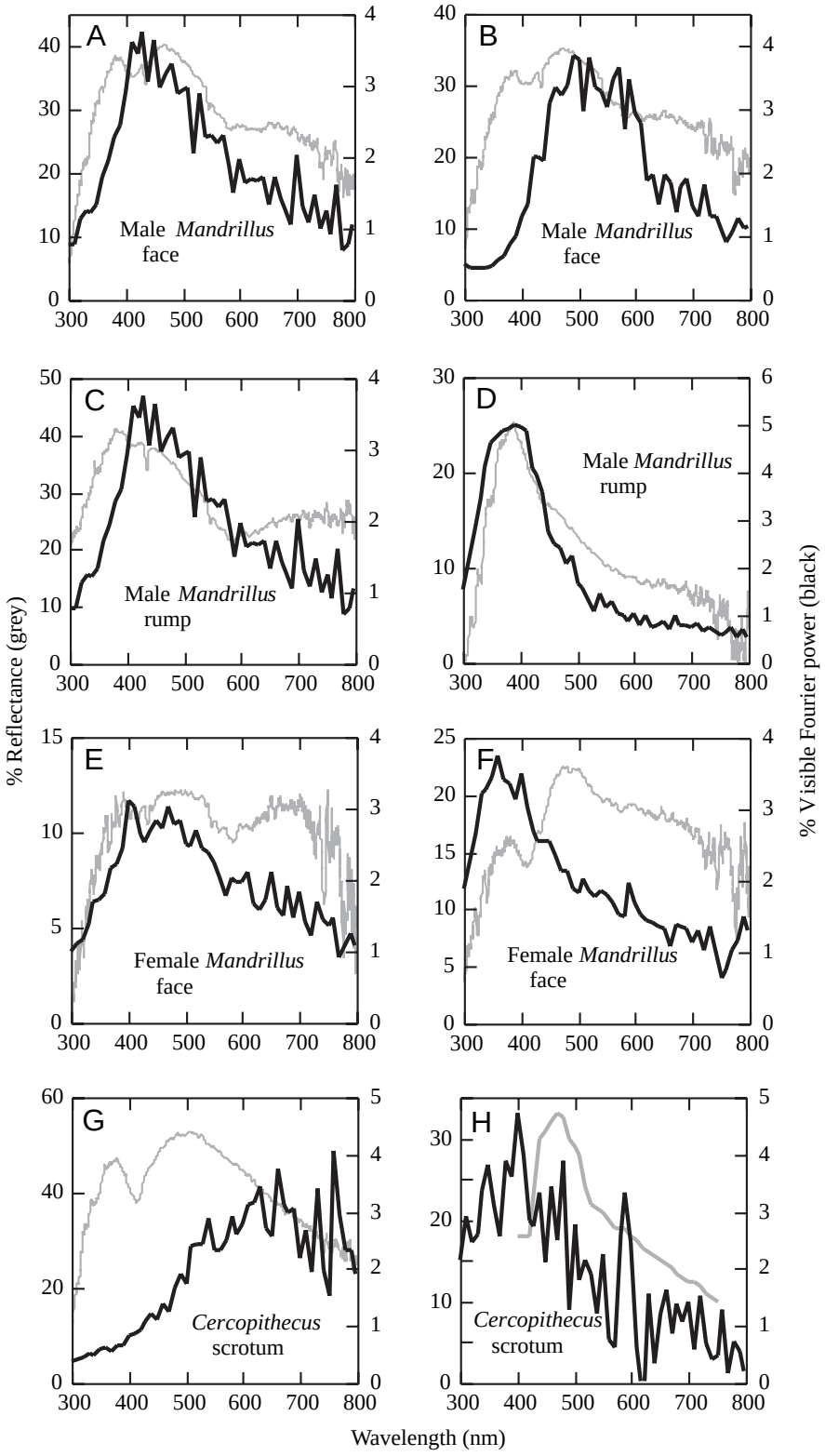

Fig. 7. Fourier predictions of the reflectance spectra (black; right axes) for different structurally coloured mammal tissues in comparison with their respective reflectance spectra (grey; left axes). (A,B) Male mandrill (*Mandrillus sphinx*) facial skin. (C,D) Male mandrill rump skin. (E,F) Female mandrill facial skin. (G) Vervet monkey (*Cercopithecus aethiops sabaeus*) 'pearly' light blue scrotum. (H) Vervet monkey (*Cercopithecus aethiops pygerythrus*) vividly blue scrotum with reflectance data from Findlay (1970). Samples A and C, and B and D were from the same individual males, respectively.

journal. To our knowledge, Oettlé (1958) was cited only twice (Findlay, 1953; Hill, 1970), and his ground-breaking results have not been followed up on until now. Price et al. (1976) subsequently used TEM to describe the distribution of melanocytes in the blue scrotal dermis of *C. aethiops* but erroneously concluded that the colour was produced by Tyndall scattering from the tissue above the melanocytes.

Evolution of collagen arrays

Colour-producing dermal collagen arrays have evolved independently in the marsupials and in the Old World primates (Cercopithecidae). Within the Old World primates, structural colours are also found in close relatives of both mandrill and vervet monkey, including on the face, genitals and rump of drill (*Mandrillus leucophaeus*), on the face of moustached monkey (*Cercopithecus cephus*) and red-bellied guenon (*Cercopithecus eyrthrogaster*) and on the scrotum and perineal region of talapoin monkey (*Miopithecus talapoin*), Patas' monkey (*Erythrocebus patas*), owl-faced monkey (*Cercopithecus hamlyni*), Dryas' monkey (*Cercopithecus dryas*), L'Hoest's monkey (*Cercopithecus lhoesti*), sun-tailed monkey (*Cercopithecus solatus*), Pruess's guenon (*Cercopithecus pruessi*) and diana monkey (*Cercopithecus diana*) (Kingdon, 1974; Gerald, 2001). *Mandrillus* and *Cercopithecus* are not hypothesized to be phylogenetically most closely related among Old World primates (Purvis, 1995; Page and Goodman, 2001), so there is a distinct likelihood that structurally coloured skin has evolved at least twice within the Old World primates. In addition to the New World didelphids *Marmosa* and *Caluromys*, blue scrotum skin is also known from the Australian dasyurid *Planigale maculata* (J. Kirsh, personal communication). This phylogenetic distribution implies that structurally coloured skin probably evolved two or more times in the marsupials. A thorough, comparative, phylogenetic survey of the distribution of structural colouration in marsupials and Old World primates is required to determine how many times this feature has evolved independently in each clade.

Interestingly, marsupials and Old World primates are the only two clades of mammals that are known to have

trichromatic colour vision. Most mammals are dichromats with poor colour sensitivity (Sumner and Mollon, 2003; Surridge et al., 2003). Trichromatic colour vision in marsupials is reported from New World opossums (Didelphidae; Freidman, 1967) and from Australian diprotodonts and polyprotodonts (Arrese et al., 2002). This phylogenetically broad sample covers the entire diversity of the marsupials, implying that a diverse group of marsupials has retained three of the four colour visual pigments (along with oil droplets and double cones) that are primitive to the vertebrates (Arrese et al., 2002). Trichromatic colour vision has reevolved in Old World primates through the duplication and sequence divergence of the X-linked opsin genes (Sumner and Mollon, 2003; Surridge et al., 2003). A fascinating stable polymorphism in X-linked opsin genes in some New World primates produces trichromacy in heterozygous females only (Surridge et al., 2003).

The evolution of structurally coloured skin only within mammalian lineages that have advanced, trichromatic colour vision supports the hypothesis that these integumentary colours function in intraspecific communication (see Function of mammalian structural colours).

Darwin (1871) concluded that: "*No other mammal is coloured in so extraordinary a manner as the adult male mandrill*", whose colours "*compare with those of the most brilliant birds*." Indeed, his apt comparison turns out to be anatomically, nanostructurally and physically accurate. Identical colour-producing collagen arrays have evolved convergently in the structurally coloured skin of many birds (Prum et al., 1999a; Prum and Torres, 2003a). Structurally coloured collagen has also evolved in the fibrous tapetum lucidum of the sheep eye (Bellairs et al., 1975) and in the iridescent corneal stroma of a variety of fishes (Lythgoe, 1974). Prum and Torres (2003a) hypothesized that colour-producing collagen arrays have evolved frequently because collagen has several intrinsic features that predispose it to evolve colour-producing nanoperiodicity. Collagen occurs as an extracellular array of fibres with a given diameter and interfibre spacing. Furthermore, collagen has a distinct refractive index (1.42) from the mucopolysaccharide matrix between the fibres (1.35). Colour-producing collagen arrays could evolve merely by specifying more rigidly the appropriate fibre sizes and distances between fibres and by producing enough fibres to create a visible colour. Also, the function of collagen in stabilizing the skin and other structures can dictate that these fibres tend to be parallel to the incident light and appropriately oriented to produce visible reflections. Structurally coloured dermal collagen arrays have probably evolved more frequently in birds than in mammals because colour vision is ubiquitous in birds. Further, avian tetrachromatic visual systems would be sensitive to a greater range of the incidental variations in collagen nanostructure that could produce coherent scattering, creating more opportunities for evolution of heritable optical variations in collagen nanostructure.

The convergent evolution of coherently scattering dermal collagen arrays in mammals and birds is also associated in both groups with the evolutionary loss of dermal iridophores (Oliphant et al., 1992). Iridophores are pigment cells that include purine or pterine crystals that produce structural colours. Dermal iridophores are primitively present in bony fishes, amphibians and reptiles but have been lost in mammals and birds (Oliphant et al., 1992). Oliphant et al. (1992) hypothesized that the evolution of hair and feathers, in mammals and birds, respectively, which covered the skin entirely, consequently led to the loss of iridophore expression in mammal and bird skin. Interestingly, some birds retain structural colour-producing iridophores in the iris of their eyes (Oliphant et al., 1992).

Melanin and structural colour production

It has been frequently suggested that melanin plays a direct role in the production of structural colours in mammalian skin (Camichel and Mandoul, 1901; Findlay, 1953, 1970; Fox, 1976; Price et al., 1976; Rees and Flanagan, 1999). Our analyses demonstrate that the structural colours are actually produced by the superficial collagen nanostructures above the typical layer of melanocytes. The function of the underlying melanosomes is to absorb light waves that are transmitted through the superficial colour-producing collagen. Without the melanin layer, these transmitted waves could scatter incoherently from tissues below that are not nanostructured to create saturated hues. This incoherent reflection could create a bright, white background reflectance that would obscure the more superficial structural colour. This function explains why these dermal structural colours can disappear if the underlying melanin layer is removed in either mammals (Findlay, 1970) or birds (Hays and Habermann, 1969). Thus, melanin pigmentation does not function directly in the production of these dermal structural colours, but melanin pigmentation can have a critical function in the effective presentation and saturation of these structural colours.

Substantial underlying melanin deposits were observed in *Cercopithecus* and *Marmosa* and in *Mandrillus* rump skin, but melanin deposition was absent from the *Mandrillus* facial skin and limited in *Caluromys*. How can *Mandrillus* facial skin and *Caluromys* scrotum produce a saturated structural colour without underlying melanin? The only other way to overcome the problem of incoherent white scattering from underlying tissues is to have so many coherently scattering objects that essentially all of the incident light is constructively reflected (Prum and Torres, 2003a). For perpendicularly incident light, reflectance (or the proportion of ambient light scattered at a single interface between two materials of different refractive indices) is calculated by the Fresnel equation to be:

$$R = [(n_D – n_A)/(n_D + n_A)]^2 ,$$

where n_D and n_A are the refractive indices of the two materials (Huxley, 1968; Land, 1972). For other pairs of materials that produce biological structural colours, R varies but is above 2 – 4.8% (chitin–air), 2.5% (guanine–water) and 4.5% (keratin–air) (Land, 1972). Theoretically, high-R array materials can produce nearly 100% coherent scattering of all ambient light at the peak wavelength of reflectance with 10–20

layers of light-scattering objects (Land, 1972). However, the difference in refractive index between collagen (n=1.42) and the mucopolysaccharide (n=1.35) is very small, yielding an R of ~0.05%. Thus, two orders of magnitude more objects are required to produce the same magnitude of reflectance with collagen arrays as with other common types of colour-producing arrays. This physical limit means that collagen arrays must be much more extensive than arrays of other materials to produce the same magnitude of reflection.

As one would predict from this relationship, the colour-producing collagen layer in male *Mandrillus* facial skin, which lacks melanin deposition, is nearly twice as thick (~1500 μm) as that in *Mandrillus* rump skin (800 μm), which has a solid melanin layer (Fig. 2A,B; Table 1). With 1500 μm of nanostructured collagen and approximately 150 nm between neighbouring fibre centres (the average of *Mandrillus* facial skin; Table 1), *Mandrillus* facial skin may be as many as 10 000 coherently scattering collagen fibres thick. This number of arrays should produce a saturated structural colour with a very low-R material. Prum and Torres (2003a) documented an anatomically similar situation in the bare-throated bellbird, *Procnias nudicollis* (Cotingidae, Aves), in which the colour-producing collagen layer (500–1000 μm) was 2–5 times thicker than in other avian species that had underlying melanin deposits.

The absence of underlying melanin creates in *Mandrillus* facial skin a potential relationship between the saturation of the colour (purity of hue) and the thickness of the tissue (i.e. the number of coherently scattering objects). Such a system can create interesting opportunities for the development and evolution of sexual dimorphism and status signalling function in the tissue (see Function of mammalian structural colours).

Dermal melanization may actually foster the evolution of structural colouration because it will render any changes in collagen nanostructure that produce coherent scattering of visible colours immediately observable (Prum and Torres, 2003a). Dermal melanin deposition is common in many Old World primates and may have preceded the evolution of structural colouration in *Mandrillus* and *Cercopithecus*. Some evidence exists that melanin deposition in mammal scrota functions to protect male germinal tissue from harmful ultraviolet radiation (Kermott and Timm, 1988). Thus, scrotal melanin deposition for radiation insulation may foster the evolution of structural colouration of the scrotum for a signal function, which has occurred independently in lineages of both marsupials and primates.

Function of mammalian structural colours

The exclusive occurrence of structural colours in mammal lineages that see visible colours strongly supports the hypothesis that these colours function in intraspecific communication and not in crypsis or interspecific communication. Darwin (1871) first hypothesized that the sexually dimorphic structural colours of primates evolved through sexual selection.

In three of the four species examined, the structural colours are restricted to the scrotum, whereas in *M. sphinx* the structural colours are found on the face, rump, perineal and genital surfaces. This patently nonrandom pattern of structural colour distribution on the bodies of mammals is probably a result of convergent sexual or social selection on scrotum colour itself, or because of a pre-existing bias in the probability of evolving a structurally coloured scrotum, perhaps because of pre-existing scrotal melanization (see above).

In solitary marsupials, a blue scrotum may function in visual recognition of males or in female mate choice. In the highly social Old World primates, structural colours function in both intersexual and intrasexual communication. In *C. aethiops*, the intensity of the blue scrotum colour varies geographically among subspecies, being most intense in the East African *C. a. pygerythrus* and least intense in the West African *C. a. sabaeus*. Hue and saturation of scrotum colour also vary substantially among individuals within *C. a. sabaeus* populations (Kingdon, 1974; Gerald, 2001) but apparently vary much less among adults in *C. a. pygerythrus* (Henzi, 1985).

In *C. a. pygerythrus*, the blue scrotum is displayed to conspecific males and females during a variety of agonistic, dominance and intergroup territorial displays (Struhsaker, 1967; Henzi, 1985). The blue scrotum is featured prominently in the ‘red-white-and-blue’ display that combines the bright red penis, the white belly fur and skin and the blue scrotum; in the red-white-and-blue display, a dominant male walks around a submissive male with his tail raised, displaying his blue scrotum (Struhsaker, 1967). Sometimes during the red-white-and-blue-display, a male stands upright with his erect penis bobbing up and down (Struhsaker, 1967). The red colour of the penis (Fig. 1C,D) is probably produced by capillary blood. The frequency of performance of the red-white-and-blue display is correlated with dominance and mating success (Struhsaker, 1967).

Gerald (2001) has demonstrated experimentally that the intensity of scrotum colour can function as a signal of social status in captive male *C. a. sabaeus*, and Gerald (1999) has also shown that blue colour is positively associated with neuroendocrine indicators of dominance. Henzi (1985) concluded that blue scrotum colour in *C. a. pygerythrus* does not vary significantly with dominance status, but Isbell (1995) presented a nonsignificant trend supporting a positive correlation between colour and status. Unfortunately, Henzi (1985) did not measure scrotal colour, and Isbell (1995) scored scrotal colour by eye with a rather ambiguous four category scale. In summary, blue scrotum structural colouration in *C. aethiops* probably functions in intrasexual and intersexual communication and probably evolved through intramale competition for status and sexual access and female preference. Additional studies are required to document how variation in scrotal colour (i.e. reflectance spectrum) functions in *Cercopithecus* populations and the mechanistic basis of that variation (see below).

M. sphinx and its sister species *M. leucophaeus* have the most complex and elaborate structural colouration in mammals. *Mandrillus* have structurally coloured patches in

both sexes and on their faces and rump, perineal and genital areas. Thus, these structural colours have the capacity to signal to a conspecific when an individual is coming or going – oriented toward or moving away from the receiver. These ubiquitous signals have complex functions within such highly social, group-living primates (Grizmek, 1984). Development of mature structural colouration occurs during puberty (4–5 years of age; Wickings and Dixson, 1992). Bright facial and rump structural colours in male *M. sphinx* have been positively correlated with plasma testosterone levels, testis size and social dominance rank (Wickings and Dixson, 1992). DNA fingerprinting analyses have demonstrated that bright male structural colours in *Mandrillus* also correlate with mating success and genetic fitness (Dixon et al., 1993; Wickings et al., 1993). Setchell and Dixson (2001) concluded that blue colouration in *Mandrillus* is unchanged by changes in alpha status. However, observations of the two 12- and 20-year-old captive male *Mandrillus* that were examined in this study contradict that conclusion. The older male was dominant in the hierachy of this captive group for many years but was deposed 4 years prior to tissue sampling by the younger male (J. Peterson and G. Nachel; personal communication). After losing his dominant status, the older male lost a substantial amount of weight and a lot of his structural colouration (J. Peterson and G. Nachel; personal communication). By the time of sampling, he was brighter again and occasionally confronting the younger dominant male in the group (J. Peterson and G. Nachel; personal communication). In conclusion, *M. sphinx* structurally coloured signals probably function in status signalling, intrasexual competition and intersexual selection.

Using a detailed model of trichromatic cercopithecine vision and measures of reflectance spectra, Sumner and Mollon (2003) have shown that the structural blue colours of *Mandrillus* and *Cercopithecus* are conspicuous against the background colours of their respective environments. Kingdon (1974) hypothesized that the evolution of blue structural colouration in Old World primates is associated with ground living, since it is found in the ground-living mandrill, drill, vervet, Patas' and moustached monkeys but is absent from some closely related, arboreal cercopithecines. However, this hypothesis is not strongly supported by a comparative survey of primate colours (Gerald, 2003) and should be tested phylogenetically.

Because of the lack of melanin underlying the colour-producing collagen arrays in the face of *Mandrillus*, changes in brilliance and saturation of the *Mandrillus* facial colour may be accomplished by expanding the thickness of the colour-producing collagen arrays. Fewer arrays would produce a colour of the same hue (peak reflectance) but with lower brilliance and saturation (less bright, more white; e.g. Fig. 3E,F) because fewer collagen fibres would create fewer opportunities to coherently scatter incident light above the white reflectance of the underlying tissue. More arrays would produce a more brilliant and saturated blue (Fig. 3A,B). Lack of underlying melanin would make colour brilliance and saturation highly sensitive to tissue thickness. Interestingly, maturation of sexually dimorphic differences in facial colouration in *M. sphinx* are associated with the development of the facial grooves that indicate the thickness of the colour-producing facial skin. Furthermore, the reflectance spectrum of the facial skin from one female *Mandrillus* showed a real lack of saturation (Fig. 3E) even though the tissue specimen from that individual showed collagen nanostructure that was virtually identical to that of the mature males (Fig. 7A,C,E). So, in *Mandrillus* facial skin, which lacks an underlying melanin layer, tissue thickness may play a direct role in development of sexual dimorphism and individual variation in structural colouration. Such changes in signal properties with age or social status could be mediated by hormonal control of collagenocyte activity in the dermis. Since facial melanin deposition is probably primitive to *Mandrillus*, the absence of melanin deposition in the blue facial patches of *Mandrillus* is likely to be a derived novelty that evolved to accommodate this signalling function.

It is attractive to hypothesize that facial structural colour in *Mandrillus* or the blue scrotum colour in *Cercopithecus* are honest indicators of individual condition because of the possible relationship between thickness of the colour-producing collagen layer and colour saturation. However, collagen is a ubiquitous protein, and the additional amounts of collagen are tiny in comparison with the mass of these large animals. Thus, it appears unlikely that there are any substantial direct physiological costs to producing the *Mandrillus* or *Cercopithecus* collagen arrays. Without any direct physiological cost to production, it is difficult to support an honest indicating trait (e.g. Andersson, 1994). Furthermore, collagen is a self-assembled protein polymer, so components of the spacing of the collagen fibres are unlikely to be easily environmentally perturbable. Thus, even if structural colour intensity is associated with dominance or status, hue itself may not be a directly condition-dependent signal. The 'honesty' of structurally coloured signal is more likely to be enforced by the cost of direct physical confrontations to individuals with inappropriate signals rather than by a direct cost of the signal production itself.

Price et al. (1976) experimentally changed the blue colour of *Cercopithecus* scrotum to white by injecting water into scrotal tissue and to deep blue by compressing the scrotum tissue. They hypothesized that scrotal colour variation in *Cercopithecus* is associated with the degree of dermal hydration. However, they did not present any evidence that natural variation in hue is associated with dermal hydration. Furthermore, it is uncertain how additional hydration would affect the nanostructure of the colour-producing arrays. Further research is required to understand the mechanism underlying the variation in scrotal hue, saturation and brilliance in *Cercopithecus*. Substantial dermal oedema or dehydration would typically only occur in a primate with more threatening health problems, so it appears more likely that dermal structural colour variations are under hormonal control.

Sources of error

There are many sources of error and limitations to the Fourier method used here to analyze the colour production (Prum and Torres, 2003a,b). An advantage of the method is that the analyses are based on actual electron micrographs of the colour-producing materials and not on a few idealized measurements. The colour predictions are based directly on the available data, but the results will be influenced by many factors that affect quantitative transmission electron microscopy, including tissue shrinkage and expansion, variation in staining, fixation, etc. The method also relies upon grey-scale differentiation of materials of different refractive indices, and additional variation in staining will create noise in the analyses. In the present study, various specimens were obtained from various sources, and differences in preservation and fixation resulted in changes in the nanostructure of the materials that reduced or eliminated structural colour production. The extracellular collagen and mucopolysaccharide arrays are particularly subject to perturbation during fixation (Prum et al., 1994; Prum and Torres, 2003a).

This Fourier method does not take into account absorption or pigmentation, but neither do any of the alternative methods of analysis of structural colouration. Absorption may play a role in the slight decline in reflectance at 400 nm in some reflectance spectra (e.g. Fig. 3A,B,E–G). Remarkably similar reflectance spectra were observed in some blue bird skin, particularly in Galliformes (Prum and Torres, 2003a,b). Alternatively, this could be due to two heterogeneous size classes of colour-producing arrays in the dermis, which are each responsible for the peaks above and below 400 nm and occur in varying frequencies (e.g. Fig. 7A *vs* Fig. 7D). This phenomenon requires further investigation.

Further, our Fourier method does not take into account polarization of incident or scattered light. Nanostructures composed of arrays of parallel fibres are likely to produce highly polarized reflections composed largely of the transverse magnetic (TM) waves, in which the magnetic field is in the plane of the image and the electric field is in the perpendicular plane of the fibre direction (e.g. Joannopoulos et al., 1995). Essentially, this Fourier method constitutes an analysis of the coherent scattering of the incident TM polarized light waves only (Prum and Torres, 2003b). However, the structural colours produced by these dermal tissues are not polarized because the larger groups of collagen fibres are oriented in many different directions within the plane of the surface of the skin. The colour seen is, thus, the sum of all the polarized reflections from many collagen arrays with different orientation, which is itself unpolarized (Prum and Torres, 2003a,b).

Another source of uncertainties is errors in estimating the radial Fourier power distributions or the predicted reflectance spectra that arise from sampling the square power spectra with different numbers of radial frequency or wavelength windows. We have chosen 100 spatial frequency and 50 wavelength radial bins, or annuli, over the ranges of values of interest (optically relevant spatial frequencies and visible wavelengths). But sampling the power spectra with different numbers of bins leads to variations in the estimation of the exact position of the peak due to unavoidable sampling errors. For example, the wavelength analyses of the Fourier power spectra from *C. a. pygerythrus* scrotum produced an estimated peak reflectance of 400 nm, or 475 nm below the peak of a published reflectance spectrum for this colour (Table 1). However, the frequency analyses for the same species produced a peak spatial frequency (the inverse of the fibre-to-fibre-centre distance) of 0.00587 nm^{-1}, which would produce a peak structural colour of 477 nm (given an average refractive index of 1.4). In this instance, 100 frequency bins produced a highly accurate estimate of the peak hue, whereas the 50 visible wavelength bins produced less accuracy. There is no way to avoid these problems, except to point out that when tissues are in a good state of preservation and many images are used, the analyses appear to converge.

In summary, our results provide strong falsification of incoherent scattering hypotheses and strong support for the coherent scattering hypothesis, but further research is required to analyze all physical sources of intraspecific and interspecific variation in structural colour within mammals, particularly in marsupials.

Fourier method and photonics

Photonics, or solid-state electromagnetics (Joannopoulos et al., 1995), is a new field of physics that has only recently begun to be applied to biological structural colour production (Parker et al., 2001; Li et al., 2003; Sundar et al., 2003; Vukusic, 2003; Vukusic and Sambles, 2003). In contrast to the traditional optical method of analyzing the sum of the responses of all incident light waves, photonics applies generalized numerical methods from quantum mechanics and electronics to analyze the periodicities in refractive index of a structure and, consequently, to predict the permissible interactions of light waves with that structure (Joannopoulos et al., 1995). Photonics has produced a revolution in new technologies and has only recently begun to be applied to biological structural colouration (Parker et al., 2001; Li et al., 2003; Sundar et al., 2003; Vukusic, 2003; Vukusic and Sambles, 2003). Although the advent of biological applications of photonic methods will require a reevaluation of all biological optical methods (Prum and Torres, 2003b), here we will only briefly discuss photonics, colour-producing collagen arrays and our alternative Fourier method.

Periodic dielectric materials, or structures with periodic spatial variation in refractive index, are called ‘photonic crystals’ (Joannopoulos et al., 1995). Almost all biological structural colour-producing materials can be understood as biophotonic crystals (Vukusic and Sambles, 2003). Photonic crystals are classified based on whether they have periodic refractive index variation in one, two or three dimensions. An array of parallel dielectric rods, like dermal colour-producing mammal collagen, is a 2-D photonic crystal (Joannopoulos et al., 1995).

Most of the mathematical methods used in photonics assume a perfect spatial periodicity (Joannopoulos et al., 1995). Although such an assumption may apply to some very crystal-

like biological structures (Parker et al., 2001; Li et al., 2003; Sundar et al., 2003), these methods are not directly applicable to quasi-ordered biomaterials in which spatial periodicity is limited to the distance of neighbouring light scatterers and is not perfectly periodic, such as mammalian and avian dermal collagen arrays. However, Jin et al. (2001) have recently shown theoretically and experimentally that an 'amorphous' (= quasi-ordered) 2-D photonic crystal can produce a full photonic band gap – a range of light frequencies that will not be transmitted in any direction within the crystal. Photonic band gaps are another consequence of coherent scattering, since coherently scattered light wavelengths cannot be transmitted forward through the photonic crystal (Joannopoulos et al., 1995). So, photonic research has confirmed that quasi-ordered (= amorphous) biological arrays constitute quasi-ordered 2-D photonic crystals and that the colour production by quasi-ordered 2-D photonic crystals is produced by coherent scattering.

Our 2-D Fourier tool provides an efficient method to quantify nanoscale spatial variation in refractive index in quasi-ordered biological materials and to test alternative hypotheses of structural colour production (Prum and Torres, 2003b). In contrast to traditional optical methods, our Fourier method shares with photonic methods an explicit focus on the analysis of the spatial periodicity of refractive index variation in the material (or tissue) as a means of predicting its light-scattering properties. Thus, there are fundamental mathematical similarities between the two approaches that we are currently investigating more fully.

We would like to give special thanks to Tim Quinn for doing all the electron microscopy. Special thanks also to the individuals who obtained and donated specimens for this research: Tim Sullivan, Jay Peterson and Gail Nachel, Brookfield Zoo, Brookfield, Illinois (*Mandrillus*); Kenneth A. Soike and Gary B. Baskin, Tulane Regional Primate Research Center, Covington, Louisiana (*Cercopithecus*); Tom Alvarado and Debbie Chase, Dallas Zoo, Dallas, Texas (*Mandrillus*); and Robert M. Timm, University of Kansas Natural History Museum, Lawrence, Kansas (*Marmosa* and *Caluromys*). Thanks to Rosetta Barkely, KU Medical School, for histology slide preparation. Photos of structurally coloured skin (Fig. 1) were kindly provided by Kenneth A. Soike, Jay Peterson, Roland Kays and Louise Emmons. The manuscript was improved by comments from and communications with Louise Emmons, Melissa Gerald, Gerald Jacobs, John Kirsh, Robert Timm and two anonymous reviewers. Funds for the research were provided by grants from the National Science Foundation to the authors (DBI-0078376, DMS-0070514) and to the University of Kansas Department of Mathematics (DMS-0112375).

References

Andersson, M. (1994). *Sexual Selection.* Princeton, NJ: Princeton University Press.

Arrese, C. A., Hart, N. S., Thomas, N., Beazley, L. D. and Shand, J. (2002). Trichromacy in Australian marsupials. *Curr. Biol.* **12**, 657-660.

Bellairs, R., Harkness, M. L. and Harkness, R. D. (1975). The structure of the tapetum of the eye of the sheep. *Cell Tissue Res.* **157**, 73-91.

Benedek, G. B. (1971). Theory of transparency of the eye. *Appl. Optics* **10**, 459-473.

Bohren, C. F. and Huffman, D. R. (1983). *Absorption and Scattering of Light by Small Particles*. New York: John Wiley & Sons.

Briggs, W. L. and Henson, V. E. (1995). *The DFT*. Philadelphia, PA: Society for Industrial and Applied Mathematics.

Camichel, C. and Mandoul, H. (1901). Des colorations bleue et verte de la peau des Vertébrés. *C. R. Seances Acad. Sci.* **133**, 826-828.

Darwin, C. (1871). *The Descent of Man, and Selection in Relation to Sex*. London: John Murray.

Dixon, A. F., Bossi, T. and Wickings, E. J. (1993). Male dominance and genetically determined reproductive success in the mandrill (*Mandrillus sphinx*). *Primates* **34**, 525-532.

Findlay, G. H. (1953). The dermal melanoblast: some cytological and spectrophotometric features. *Br. J. Dermatol.* **65**, 437-447.

Findlay, G. H. (1970). Blue skin. *Br. J. Dermatol.* **83**, 127-134.

Fox, D. L. (1976). *Animal Biochromes and Structural Colors*. Berkeley, CA: University of California Press.

Freidman, H. (1967). Colour vision in the Virginia opossum. *Nature* **213**, 835-836.

Gerald, M. S. (1999). *Scrotal Color in Vervet Monkeys (*Cercopithecus aethiops sabaeus*): the Signal Functions and Potential Proximate Mechanisms of Color Variation*. Los Angeles: University of California.

Gerald, M. S. (2001). Primate colour predicts social status and aggressive outcome. *Anim. Behav.* **61**, 559-566.

Gerald, M. S. (2003). How color can guide the primate world. In *Sexual Selection and Reproductive Competition in Primates* (ed. C. B. Jones), pp. 141-172. Washington, DC: American Society of Primatologists.

Grizmek, B. (1984). *Grizmek's Animal Life Encyclopedia*, vol. 10 *Mammals I*. New York: Van Nostrand Reinhold Company.

Hays, H. and Habermann, H. (1969). Note on bill color of the ruddy duck, *Oxyura jamaicensis rubida*. *Auk* **86**, 765-766.

Henzi, S. P. (1985). Genital signalling and the coexistence of male vervet monkeys (*Cercopithecus aethiops pygerythrus*). *Folia Primatol.* **45**, 129-147.

Herring, P. J. (1994). Reflective systems in aquatic animals. *Comp. Biochem. Physiol. A* **109**, 513-546.

Hill, W. C. (1970). *Primates – Comparative Anatomy and Taxonomy*, vol. VIII, *Cynopithecinae*. New York: John Wiley & Sons.

Huxley, A. F. (1968). A theoretical treatment of the reflexion of light by multi-layer structures. *J. Exp. Biol.* **48**, 227-245.

Isbell, L. A. (1995). Seasonal and social correlates of changes in hair, skin, and scrotal condition in vervet monkeys (*Cercopithecus aethiops*) of Amboseli National Park, Kenya. *Am. J. Primatol.* **36**, 61-70.

Jin, C., Meng, X., Cheng, B., Li, Z. and Zhang, D. (2001). Photonic gap in amorphous photonic materials. *Phys. Rev. B* **63**, 195107.

Joannopoulos, J. D., Meade, R. D. and Winn, J. N. (1995). *Photonic Crystals: Molding the Flow of Light.* Princeton, NJ: Princeton University Press.

Kermott, L. H. and Timm, R. M. (1988). Scrotal melanins in bats (Chiroptera): description, distribution, and function. *J. Zool.* **214**, 519-532.

Kingdon, J. (1974). *East African Mammals.* Chicago, IL: Chicago University Press.

Land, M. F. (1972). The physics and biology of animal reflectors. *Prog. Biophys. Mol. Biol.* **24**, 77-106.

Lee, D. W. (1991). Ultrastructural basis and function of iridescent blue colour of fruits in *Elaeocarpus*. *Nature* **349**, 260-262.

Lee, D. W. (1997). Iridescent blue plants. *Am. Sci.* **85**, 56-63.

Leonard, D. W. and Meek, K. M. (1997). Refractive indices of the collagen fibrils and extrafibrillar material of the corneal stroma. *Biophys. J.* **72**, 1382-1387.

Li, J., Yu, X., Hu, X., Xu, C., Wang, X., Liu, X. and Fu, R. (2003). Coloration strategies in peacock feathers. *Proc. Natl. Acad. Sci. USA* **100**, 12576-12578.

Lythgoe, J. N. (1974). The structure and phylogeny of iridescent corneas in fishes. In *Vision in Fishes: New Approaches in Research* (ed. M. A. Ali), pp. 253-262. New York: Plenum Press.

Mason, C. W. (1923). Structural colors of feathers. I. *J. Phys. Chem.* **27**, 201-251.

Maurice, D. M. (1984). The cornea and sclera. In *The Eye* (ed. H. Davson), pp. 1-158. New York: Academic Press.

Nassau, K. (1983). *The Physics and Chemistry of Color*. New York: John Wiley & Sons.

Neville, A. C. and Caveney, S. (1969). Scarabaeid beetle exocuticle as an optical analogue of cholesteric liquid crystals. *Biol. Rev.* **44**, 531-562.

Oettlé, A. G. (1958). The blue scrotum of the vervet monkey. *S. Afr. J. Med. Sci.* **23**, 225-230.

Oliphant, L. W., Hudon, J. and Bagnara, J. T. (1992). Pigment cell refugia in homeotherms – the unique evolutionary position of the iris. *Pigment Cell Res.* **5**, 367-371.

Page, S. L. and Goodman, M. (2001). Catarrhine phylogeny: noncoding DNA evidence for a diphyletic origin of the mangabeys and for a human–chimpanzee clade. *Mol. Phylogen. Evol.* **18**, 14-25.

Parker, A. R. (1999). Invertebrate structural colours. In *Functional Morphology of the Invertebrate Skeleton* (ed. E. Savazzi), pp. 65-90. London: John Wiley & Sons.

Parker, A. R., McPhedran, R. C., McKenzie, D. R., Botten, L. C. and Nicorovici, N.-A. P. (2001). Aphrodite's iridescence. *Nature* **409**, 36-37.

Price, J. S., Burton, J. L. and Shuster, S. (1976). Control of scrotal colour in vervet monkey. *J. Med. Primatol.* **5**, 296-304.

Prum, R. O. and Torres, R. H. (2003a). Structural colouration of avian skin: convergent evolution of coherently scattering dermal collagen arrays. *J. Exp. Biol.* **206**, 2409-2429.

Prum, R. O. and Torres, R. H. (2003b). A Fourier tool for the analysis of coherent light scattering by bio-optical nanostructures. *Integ. Comp. Biol.* **43**, 591-602.

Prum, R. O., Morrison, R. L. and Ten Eyck, G. R. (1994). Structural color production by constructive reflection from ordered collagen arrays in a bird (*Philepitta castanea*: Eurylaimidae). *J. Morphol.* **222**, 61-72.

Prum, R. O., Torres, R. H., Williamson, S. and Dyck, J. (1998). Coherent light scattering by blue feather barbs. *Nature* **396**, 28-29.

Prum, R. O., Torres, R. H., Kovach, C., Williamson, S. and Goodman, S. M. (1999a). Coherent light scattering by nanostructured collagen arrays in the caruncles of the Malagasy asities (Eurylaimidae: Aves). *J. Exp. Biol.* **202**, 3507-3522.

Prum, R. O., Torres, R. H., Williamson, S. and Dyck, J. (1999b). Two-dimensional Fourier analysis of the spongy medullary keratin of structurally coloured feather barbs. *Proc. R. Soc. Lond. B* **266**, 13-22.

Prum, R. O., Andersson, S. and Torres, R. H. (2003). Coherent scattering of ultravioltet light by avian feather barbs. *Auk* **120**, 163-170.

Purvis, A. (1995). A composite estimate of primate phylogeny. *Phil. Trans. R. Soc. Lond. B* **348**, 405-421.

Rees, J. L. and Flanagan, N. (1999). Pigmentation, melanocortins and red hair. *QJM* **92**, 125-131.

Reisfeld, P. L. (2000). Blue in the skin. *J. Am. Acad. Dermatol.* **42**, 597-605.

Setchell, J. M. and Dixson, A. F. (2001). Changes in secondary sexual adornments of male mandrills (*Mandrillus sphinx*) are associated with gain and loss of alpha status. *Hormones Behav.* **39**, 177-184.

Srinivasarao, M. (1999). Nano-optics in the biological world: beetles, butterflies, birds, and moths. *Chem. Rev.* **99**, 1935-1961.

Struhsaker, T. T. (1967). Behavior of vervet monkeys (*Cercopithecus aethiops*). *Univ. California Publ. Zool.* **82**, 1-64.

Sumner, P. and Mollon, J. D. (2003). Colors of primate pelage and skin: objective assessment of conspicuousness. *Am. J. Primatol.* **59**, 67-91.

Sundar, V. C., Yablon, A. D., Grazul, J. L., Ilan, M. and Aizenberg, J. (2003). Fibre-optical features of a glass sponge. *Nature* **424**, 899-900.

Surridge, A. K., Osorio, D. and Mundy, N. I. (2003). Evolution and selection of trichromatic vision in primates. *Trends Ecol. Evol.* **18**, 198-205.

Vukusic, P. (2003). Natural coatings. In *Optical Interference Coatings* (ed. N. Kaiser and H. K. Pulker), pp. 1-34. Berlin: Springer-Verlag.

Vukusic, P. and Sambles, J. R. (2003). Photonic structures in biology. *Nature* **424**, 852-855.

Wickings, E. J., Bossi, T. and Dixson, A. F. (1993). Reproductive success in the mandrill, *Mandrillus sphinx*: correlations of male dominance and mating success with paternity, as determined by DNA fingerprinting. *J. Zool. Lond.* **231**, 563-574.

Wickings, E. J. and Dixson, A. F. (1992). Testicular function, secondary sexual development, and social status in male mandrills (*Mandrillus sphinx*). *Physiol. Behav.* **52**, 909-916.

Young, A. T. (1982). Rayleigh Scattering. *Physics Today* **35**, 42-48.